Rapid Communications

Experimental realization of a feedback optical parametric amplifier with four-wave mixing

Xiaozhou Pan,[1] Hui Chen,[2] Tianxiang Wei,[1] Jun Zhang,[2,*] Alberto M. Marino,[3] Nicolas Treps,[4]
Ryan T. Glasser,[5] and Jietai Jing[1,6,7,†]

[1]*State Key Laboratory of Precision Spectroscopy, School of Physics and Materials Science, East China Normal University, Shanghai* 200062, *China*

[2]*UMich-SJTU Joint Institute, Key Laboratory of System Control and Information Processing (MOE), Shanghai Jiao Tong University, Shanghai,* 200240, *China*

[3]*Homer L. Dodge Department of Physics and Astronomy, University of Oklahoma,* 440 *West Brooks Street, Norman, Oklahoma* 73019, *USA*

[4]*Laboratoire Kastler Brossel, Sorbonne Universités UPMC, École Normale Supérieure, Collège de France, CNRS,* 4 *place Jussieu,* 75252 *Paris, France*

[5]*Department of Physics and Engineering Physics, Tulane University,* 6400 *Freret Street, New Orleans, Louisiana* 70118, *USA*

[6]*Department of Physics, Zhejiang University, Hangzhou* 310027, *China*

[7]*Collaborative Innovation Center of Extreme Optics, Shanxi University, Taiyuan, Shanxi* 030006, *China*

(Received 5 September 2017; published 26 April 2018)

Optical parametric amplifiers (OPAs) play a fundamental role in the generation of quantum correlation for quantum information processing and quantum metrology. In order to increase the communication fidelity of the quantum information protocol and the measurement precision of quantum metrology, it requires a high degree of quantum correlation. In this Rapid Communication we report a feedback optical parametric amplifier that employs a four-wave mixing (FWM) process as the underlying OPA and a beam splitter as the feedback controller. We first construct a theoretical model for this feedback-based FWM process and experimentally study the effect of the feedback control on the quantum properties of the system. Specifically, we find that the quantum correlation between the output fields can be enhanced by tuning the strength of the feedback.

DOI: 10.1103/PhysRevB.97.161115

An optical parametric amplifier (OPA) is a fundamental device in quantum optics to generate and manipulate quantum optical fields in both continuous [1–13] and discrete variable systems [14–16]. Among others, four-wave mixing (FWM) in a hot atomic vapor cell has been shown to be a promising candidate as an OPA due to its strong nonlinearity for interactions, multispatial mode nature, and natural spatial separation of the output states [17]. These features lead to many prospective applications for FWM as an OPA in quantum information processing [18–25] and quantum metrology [26–28]. In order to increase the communication fidelity of the quantum information protocol and the measurement precision of quantum metrology, it requires a high degree of quantum correlation. Feedback control is an important concept of modern technology. Generally, it occurs when outputs of a system are routed back as inputs of itself. It has been applied to not only classical dynamical systems [29,30], but also quantum systems [31,32] to increase stability margins, enhance robustness to model uncertainties and parameter variations, and reduce noise distortions [33,34]. In this Rapid Communication, we present the experimental implementation of a feedback optical parametric amplifier (FOPA). It combines FWM in the hot atomic vapor cell as the OPA with a beam splitter (BS) with tunable reflectivity as the feedback controller. We demonstrate that the quantum correlation between the output fields can be manipulated or even enhanced by changing the feedback strength. Moreover, we calculate the quantum correlation by using a theoretical model of the FOPA and show that the numerical results are consistent with the experimental data.

The conceptual model of our FOPA is illustrated in Fig. 1(a), similar to the prototype proposed for system gain stabilization [35]. Our experimental scheme is shown in Fig. 1(b) where a FWM process is used as the OPA (A) and a tunable BS as the controller (C). The OPA with pump power P is seeded by a coherent state in mode $\hat{a}_1$, and the BS controller with reflectivity of k controls the feedback path by feeding part of the output field $\hat{b}_2$ back into the other input port of the OPA. Let us represent the scattering matrix of the OPA as

$$A = \begin{bmatrix} \sqrt{G} & \sqrt{G-1} \\ \sqrt{G-1} & \sqrt{G} \end{bmatrix}, \tag{1}$$

where G is the gain of the OPA [36] and the scattering matrix of the controller is as follows:

$$C = \begin{bmatrix} \sqrt{1-k} & \sqrt{k} \\ -\sqrt{k} & \sqrt{1-k} \end{bmatrix}, \tag{2}$$

where k is the reflectivity of the BS controller. Note that, for ease of analysis, we use the gain for the FWM model instead of the pump power as in the experimental part. Experimentally, the gain G can be directly measured for a given pump power. The relation between two inputs $(\hat{a}_1, \hat{v}_1)$ and two outputs $(\hat{b}_1, \hat{d}_1)$ of the feedback system can be obtained by eliminating

*Corresponding author: zhangjun12@sjtu.edu.cn
†Corresponding author: jtjing@phy.ecnu.edu.cn

 ©2018 American Physical Society

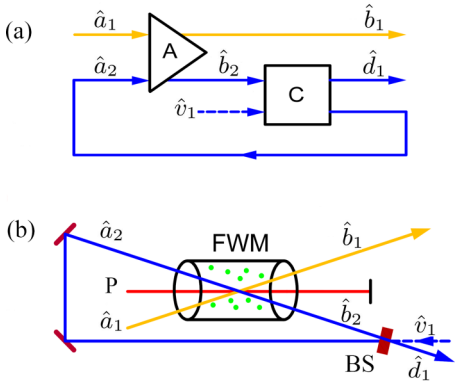

FIG. 1. (a) A theoretical model of FOPA, where A is the OPA and C is the feedback controller. (b) The experimental scheme for the FOPA consists of a FWM process in a hot atomic vapor cell as the OPA and a tunable BS as the controller.

the intermediate operators $\hat{a}_2$ and $\hat{b}_2$,

$$\begin{bmatrix} \hat{b}_1 \\ \hat{d}_1^\dagger \end{bmatrix} = \frac{1}{1+\sqrt{G}ke^{-i\phi}} \begin{bmatrix} g_{11} & g_{12} \\ g_{21} & g_{22} \end{bmatrix} \begin{bmatrix} \hat{a}_1 \\ \hat{v}_1^\dagger \end{bmatrix}, \tag{3}$$

where

$$g_{11} = \sqrt{G} + \sqrt{k}e^{-i\phi}, \quad g_{12} = e^{-i\phi}\sqrt{(1-k)(G-1)}, \tag{4}$$

$$g_{21} = \sqrt{(G-1)(1-k)}, \quad g_{22} = \sqrt{G}e^{-i\phi} + \sqrt{k}, \tag{5}$$

and ϕ is the phase delay introduced by the feedback path. The photon number sum operator of the probe and conjugate beams is

$$\hat{N} = \hat{b}_1^\dagger \hat{b}_1 + \hat{d}_1^\dagger \hat{d}_1, \tag{6}$$

and the difference is

$$\hat{Z} = \hat{b}_1^\dagger \hat{b}_1 - \hat{d}_1^\dagger \hat{d}_1. \tag{7}$$

The quantum correlation of the output fields of our FOPA can be characterized by the degree of the intensity difference squeezing (IDS) of the two output fields which is defined as [37]

$$S = \frac{\mathrm{Var}(\hat{Z})}{\langle \hat{N} \rangle}. \tag{8}$$

Figure 2(a) shows the detailed experimental setup of the FOPA in which the OPA is based on a FWM process in a double-Λ configuration in a ^{85}Rb vapor cell as shown in Fig. 2(b). The ^{85}Rb cell is 12-mm long, and its temperature is stabilized around 116 °C. The laser beam from a cavity-stabilized Ti:sapphire laser is split into two parts where one acts as the pump beam for the FWM process and the other acts as the input seed Pr after double passing through an AOM. These two beams are then combined with PBS1 such that they cross each other at the center of the ^{85}Rb cell at a small angle of around 7 mrad. The waists of the pump and probe beams at the center of the ^{85}Rb cell are 675 and 395 μm, respectively.

After the FWM process, PBS2 is used to filter out the pump beam, and the probe beam is directed into a photodiode (D1) with a high reflectivity mirror (M1). Meanwhile, a Conj is generated, which is then split into two beams by a C consisting of HWP1 and PBS3. The beam going through the PBS3 is incident on D2, whereas the reflected portion is injected into the unused input port of the FWM process. HWP2 is used to rotate the polarization of the conjugate beam from vertical to horizontal in order to keep the same polarization as the injected probe beam. Two lenses L1 and L2 with focal lengths of 500 mm are used in a $4F$ imaging configuration inside the feedback loop with total length of around 2 m to ensure that the waist of the conjugate beam is reproduced at the center of the vapor cell. This is critical for constructing an efficient feedback control loop.

By rotating the HWP1 and thus changing the intensity of the reflected portion of the conjugate beam, we can control the feedback ratio k. When $k = 0$, all the conjugate beams go through PBS3, and the FOPA reduces to a traditional phase-insensitive FWM, i.e., the OPA. In general, a nonzero k yields a two-port seeded phase-sensitive FWM amplifier [38,39]. We use the coherent modulation locking technique [40] to maximize the intensities of the output fields via mirrors mounted PZT1 and PZT2.

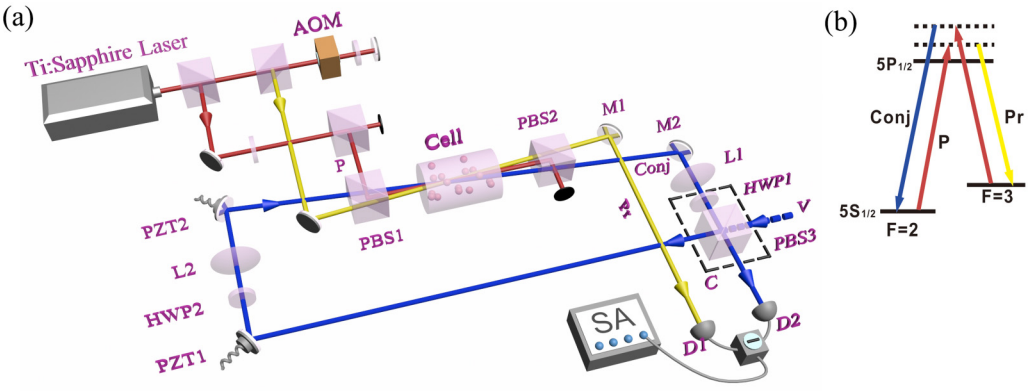

FIG. 2. Experimental setup of the FOPA. (a) A Ti:sapphire laser: the main laser; AOM: acousto-optic modulator; PBS1–PBS3: polarizing beam splitters; Cell: hot ^{85}Rb vapor cell; M1 and M2: mirrors; L1 and L2: lenses; PZT1 and PZT2: piezoelectric transducers; D1 and D2: photodetectors; SA: spectrum analyzer; HWP1 and HWP2: half-wave plates; C: feedback controller consists of HWP1 and PBS3; V: vacuum field. (b) Energy-level diagram of the double-Λ scheme in the D1 line of ^{85}Rb. P: pump beam; Pr: probe beam; Conj: conjugate beam.

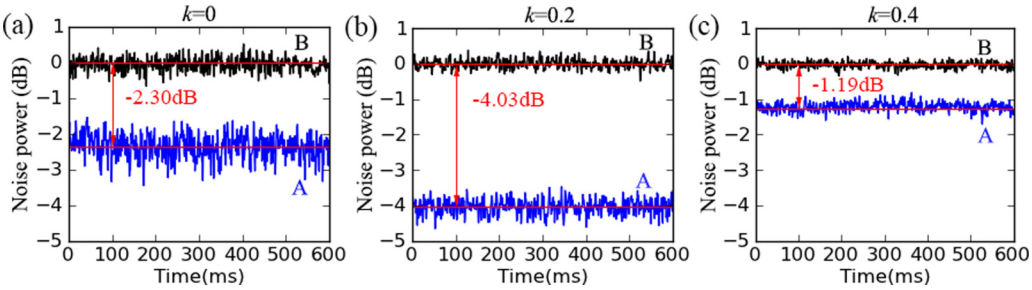

FIG. 3. Three typical feedback results for a pump power of 85 mW and a probe power of 30 μW. (a)–(c) are the normalized noise power of the intensity difference for the twin beams generated by the FOPA (blue traces A) and the corresponding SNLs (black traces B) with $k = 0$, 0.2, and 0.4, respectively. The straight red lines are the mean values for the corresponding traces.

To investigate the effect of the controller on quantum properties of the system, we characterize the quantum correlations through measurements of the IDS between the two output fields $\hat{b}_1$ and $\hat{d}_1$ in Fig. 1 (i.e., probe and conjugate beams in Fig. 2). To measure the IDS in experiment, we use D1 and D2 with a quantum efficiency of around 96% that are integrated into a single balanced photodetector with transimpedance gain of 10^5 V/A. The IDS can then be obtained by comparing the variance of the photocurrent difference between D1 and D2 with the corresponding shot-noise limit (SNL) [37]. We calibrate the SNL by using a beam in a coherent state with a power equal to the total power of the output fields $\hat{b}_1$ and $\hat{d}_1$ incident on D1 and D2. Then we split it with a 50:50 BS and direct the obtained beams to D1 and D2 to record the noise power of the intensity difference between the two output fields. For a given k, we measure the noise power of the intensity difference as well as the corresponding SNL with a SA set to 30-kHz resolution bandwidth, 300-Hz video bandwidth, zero span, and a center frequency of 2 MHz.

We show that the feedback ratio k can change or even enhance the quantum correlation. For $k = 0$, 0.2, and 0.4, we plot the normalized noise power of the intensity difference in Fig. 3 with the powers of the probe and pump beams set to 30 μW and 85 mW, respectively. The black traces B averaged at 0 dB give the SNLs taken as references, and the blue traces A give the noise powers of the intensity difference between the two output fields. In all these cases, the normalized noise power of the intensity difference is below the corresponding SNL, indicating the presence of squeezing. When $k = 0$, as shown in Fig. 3(a), we see that the average IDS is -2.30 dB. This corresponds to the FWM process with no feedback. When $k = 0.2$, as shown in Fig. 3(b), a squeezing of -4.03 dB is observed, showing a clear enhancement of squeezing over the no feedback case. However, when further increasing the value of k to 0.4 as in Fig. 3(c), we observe a squeezing of -1.19 dB, which shows that the quantum correlation is decreased by excessive feedback.

Furthermore, we study the optimal feedback ratio k^* that maximizes the quantum correlation. Figure 4 shows the IDS of the output fields as we sweep the feedback ratio k from 0, 0.1, 0.15, 0.20, 0.25, 0.3, 0.35, 0.4, to 0.45, for pump powers of 65, 75, and 85 mW, respectively. It is clear that there exists a k^* that maximizes the quantum enhancement of the system. We find that when $P = 65$ mW, k^* lies in [0.25,0.35] and the IDS is -2.65 dB; when $P = 75$ mW, k^* is in [0.20,0.30] and the IDS is -3.54 dB; and when $P = 85$ mW, k^* is in [0.15,0.25] and the IDS is -4.03 dB. From additional measurements at other pump powers, we find that the higher the pump power is, the smaller k^* becomes. This is also confirmed with the theoretical analysis presented in the Supplemental Material [41].

The existence of an optimal feedback ratio can be explained by the interplay of two mechanisms. The first one is the feedback mechanism that comes from the recycling of the conjugate beam on the feedback path and thus enhances the quantum properties of the FOPA. The other is the vacuum noise mechanism that comes from the unused port of the controller ($\hat{v}_1$ in Fig. 1), which deteriorates the quantum properties of the output states. When k is small, the quantum correlation degradation caused by vacuum noise is low, and the feedback mechanism dominates and leads to an increase in the total quantum correlation. When k is increased, the effect of the vacuum noise mechanism becomes significant, and the quantum correlation is reduced as shown in Fig. 3(c). The optimal feedback ratio occurs when the effects of the two

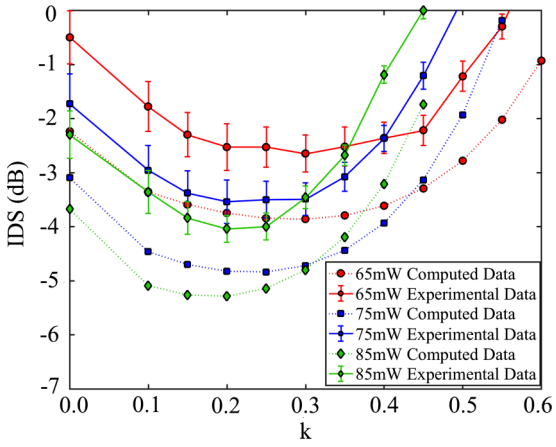

FIG. 4. IDS versus feedback ratio k with the pump power set to 65, 75, and 85 mW, respectively. The solid lines are experimental data, and the dotted lines are the computed data with the model parameters chosen as the transmission coefficients of the probe beam $T_a = 0.9$, the transmission coefficients of the conjugate beam $T_b = 0.95$, propagation loss $l = 0.18$, and detector efficiency $\eta = 0.9$ (see the Supplemental Material [41]). The red dot: 65-mW pump power; the blue square: 75-mW pump power; the green diamond: 85-mW pump power.

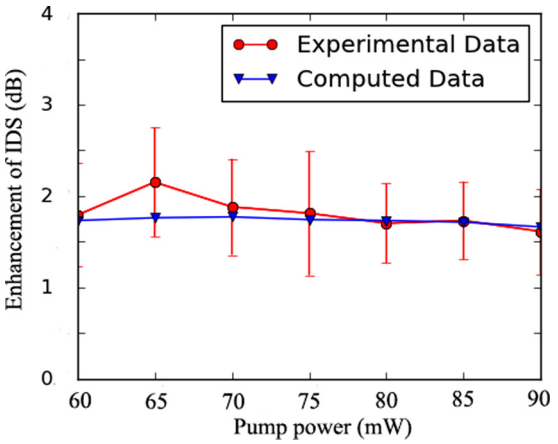

FIG. 5. Maximal enhancement of the IDS versus pump power. The red dotted line is the experimental data, and the blue triangle line is the computed data.

mechanisms balance each other, and the maximal quantum enhancement is achieved.

We now consider the theoretical analysis for the FOPA platform. We develop an input-output model for the FOPA by including three sources of losses, i.e., the FWM vapor cell's absorbing effect [36,42], propagation, and detector losses. With the input-output relation, we can compute the IDS explicitly. For details, see the Supplemental Material [41]. We plot the computed IDS and the experimental data versus k in Fig. 4. Overall, the theoretical calculation matches well with the experiments except for a constant offset of around 1.3 dB that can be further compensated by including more losses [36].

As the pump power increases, the IDSs of both the FWM with no feedback (S_{FWM}) and the FOPA at the optimal feedback ratio (S^{*}_{FOPA}) increase. To study how the maximal enhancement ($S_{\mathrm{FWM}} - S^{*}_{\mathrm{FOPA}}$) varies as the pump power is changed, we sweep the pump power in the experimentally feasible range from 60, 65, 70, 75, 80, and 85 mW to 90 mW and collect the corresponding maximal enhancements. We also numerically calculate the expected enhancements with our FOPA model and find that the theoretical results are close to the experimental ones as shown in Fig. 5. It can be observed that the quantum enhancement stays nearly the same for this range of pump powers.

In conclusion, we have experimentally implemented a FOPA that consists of a FWM process as an OPA and a BS as a controller. We demonstrate that the quantum correlation between the output fields can be enhanced by the feedback ratio. Moreover, we find an optimal feedback ratio that maximizes the quantum correlation enhancement at a given pump power. Our results show that, within the range of feasible pump powers in the laboratory, the maximal quantum correlation enhancements are almost the same. In addition, we also develop a theoretical model and performed numerical computations to corroborate the experimental observations. Our results open the way to apply the concept of feedback control strategy to other quantum optics system for the purposes of enhancing communication fidelity [43,44] of quantum information processing and measurement precision of quantum metrology [26–28].

J.J. thanks the National Natural Science Foundation of China (NSFC) (Grants No. 91436211, No. 11374104, and No. 10974057), the Natural Science Foundation of Shanghai (Grant No. 17ZR1442900), the Program of Scientific and Technological Innovation of Shanghai (Grant No. 17JC1400401), the National Basic Research Program of China (Grant No. 2016YFA0302103), and the 111 project (Grant No. B12024), the Fundamental Research Funds for the Central University; Program of State Key Laboratory of Advanced Optical Communication Systems and Networks (Grant No. 2018GZKF03006); J.Z. thanks the National Natural Science Foundation of China (NSFC) Grants No. 61174086 and No. 61533012, and the State Key Laboratory of Precision Spectroscopy, ECNU, China.

X. Pan and H. Chen contributed equally to this Rapid Communication.

[1] S. L. Braunstein and P. van Loock, Rev. Mod. Phys. **77**, 513 (2005).
[2] Z. Y. Ou, S. F. Pereira, H. J. Kimble, and K. C. Peng, Phys. Rev. Lett. **68**, 3663 (1992).
[3] J. Jing, J. Zhang, Y. Yan, F. Zhao, C. Xie, and K. Peng, Phys. Rev. Lett. **90**, 167903 (2003).
[4] S. Armstrong, J.-F. Morizur, J. Janousek, B. Hage, N. Treps, P. K. Lam, and H.-A. Bachor, Nat. Commun. **3**, 1026 (2012).
[5] M. Pysher, Y. Miwa, R. Shahrokhshahi, R. Bloomer, and O. Pfister, Phys. Rev. Lett. **107**, 030505 (2011).
[6] O. Pinel, P. Jian, R. M. de Araújo, J. Feng, B. Chalopin, C. Fabre, and N. Treps, Phys. Rev. Lett. **108**, 083601 (2012).
[7] S. Yokoyama, R. Ukai, S. C. Armstrong, C. Sornphiphatphong, T. Kaji, S. Suzuki, J.-i. Yoshikawa, H. Yonezawa, N. C. Menicucci, and A. Furusawa, Nat. Photonics **7**, 982 (2013).
[8] M. Chen, N. C. Menicucci, and O. Pfister, Phys. Rev. Lett. **112**, 120505 (2014).
[9] J. Roslund, R. M. de Araujo, S. Jiang, C. Fabre, and N. Treps, Nat. Photonics **8**, 109 (2014).
[10] S. Armstrong, M. Wang, R. Y. Teh, Q. Gong, Q. He, J. Janousek, H.-A. Bachor, M. D. Reid, and P. K. Lam, Nat. Phys. **11**, 167 (2015).
[11] R. Dong, M. Lassen, J. Heersink, C. Marquardt, R. Filip, G. Leuchs, and U. L. Andersen, Nat. Phys. **4**, 919 (2008).
[12] R. E. Slusher, L. Hollberg, B. Yurke, J. C. Mertz, and J. F. Valley, Phys. Rev. A **31**, 3512 (1985).
[13] R. E. Slusher, L. W. Hollberg, B. Yurke, J. C. Mertz, and J. F. Valley, Phys. Rev. Lett. **55**, 2409 (1985).
[14] J. Pan, Z. Chen, C. Lu, H. Weinfurter, A. Zeilinger, and M. Żukowski, Rev. Mod. Phys. **84**, 777 (2012).
[15] X. Yao, T. Wang, P. Xu, H. Lu, G. Pan, X. Bao, C. Peng, C. Lu, Y. Chen, and J. Pan, Nat. Photonics **6**, 225 (2012).
[16] S. Yang, X. Wang, X. Bao, and J. Pan, Nat. Photonics **10**, 381 (2016).

[17] C. F. McCormick, V. Boyer, E. Arimondo, and P. D. Lett, Opt. Lett. **32**, 178 (2007).
[18] A. M. Marino, R. C. Pooser, V. Boyer, and P. D. Lett, Nature (London) **457**, 859 (2009).
[19] Z. Qin, L. Cao, H. Wang, A. M. Marino, W. Zhang, and J. Jing, Phys. Rev. Lett. **113**, 023602 (2014).
[20] N. V. Corzo, Q. Glorieux, A. M. Marino, J. B. Clark, R. T. Glasser, and P. D. Lett, Phys. Rev. A **88**, 043836 (2013).
[21] C. S. Embrey, M. T. Turnbull, P. G. Petrov, and V. Boyer, Phys. Rev. X **5**, 031004 (2015).
[22] M. W. Holtfrerich, M. Dowran, R. Davidson, B. J. Lawrie, R. C. Pooser, and A. M. Marino, Optica **3**, 985 (2016).
[23] R. T. Glasser, U. Vogl, and P. D. Lett, Phys. Rev. Lett. **108**, 173902 (2012).
[24] R. M. Camacho, P. K. Vudyasetu, and J. C. Howell, Nat. Photonics **3**, 103 (2009).
[25] N. V. Corzo, A. M. Marino, K. M. Jones, and P. D. Lett, Phys. Rev. Lett. **109**, 043602 (2012).
[26] F. Hudelist, J. Kong, C. Liu, J. Jing, Z. Y. Ou, and W. Zhang, Nat. Commun. **5**, 3049 (2014).
[27] R. C. Pooser and B. Lawrie, Optica **2**, 393 (2015).
[28] N. Otterstrom, R. C. Pooser, and B. J. Lawrie, Opt. Lett. **39**, 6533 (2014).
[29] J. Bechhoefer, Rev. Mod. Phys. **77**, 783 (2005).
[30] K. Zhou, J. Doyle, and K. Glover, *Robust and Optimal Control* (Prentice Hall, Englewood Cliffs, NJ, 1996).
[31] S. Lloyd, Phys. Rev. A **62**, 022108 (2000).
[32] H. M. Wiseman and G. J. Milburn, *Quantum Measurement and Control* (Cambridge University Press, Cambridge, 2010).
[33] K. Jacobs, X. Wang, and H. M Wiseman, New J. Phys. **16**, 073036 (2014).
[34] N. Yamamoto, Phys. Rev. X **4**, 041029 (2014).
[35] N. Yamamoto, Phys. Rev. Appl. **5**, 044012 (2016).
[36] M. Jasperse, L. D. Turner, and R. E. Scholten, Opt. Express **19**, 3765 (2011).
[37] M. Fox, *Quantum Optics: An Introduction* (Oxford University Press, New York, 2006).
[38] Y. Fang and J. Jing, New J. Phys. **17**, 23027 (2015).
[39] J. Xin, H. Wang, and J. Jing, Appl. Phys. Lett. **109**, 051107 (2016).
[40] H. Wang, A. Marino, and J. Jing, Appl. Phys. Lett. **107**, 121106 (2015).
[41] See Supplemental Material at http://link.aps.org/supplemental/10.1103/PhysRevB.97.161115 for theoretical model of feedback-based FWM process with consideration of losses.
[42] C. F. McCormick, A. M. Marino, V. Boyer, and P. D. Lett, Phys. Rev. A **78**, 043816 (2008).
[43] A. Furusawa, J. L. Sørensen, S. L. Braunstein, C. A. Fuchs, H. J. Kimble, and E. S. Polzik, Science **282**, 706 (1998).
[44] H. Yonezawa, T. Aoki, and A. Furusawa, Nature (London) **431**, 430 (2004).